~~Active m~~Microbial sulfur cycling across a 13,500-year-old lake sediment record

Jasmine S. Berg[1*], Paula C. Rodriguez[2], Cara Magnabosco[2], Longhui Deng[3a], Stefano M. Bernasconi[2], Hendrik Vogel[4], Marina Morlock[4b], Mark A. Lever[3c]

[1]Institute of Earth Surface Dynamics, Department of Geosciences and Environment, University of Lausanne, 1015 Lausanne, Switzerland

[2]Department of Earth and Planetary Sciences, ETH-Zurich, 8049 Zurich, Switzerland

[3]Institute of Biogeochemistry and Pollutant Dynamics, Department of Environmental Systems Science, ETH-Zurich, 8049 Zurich, Switzerland

[4]Institute of Geological Sciences & Oeschger Centre for Climate Change Research, University of Bern, 3012 Bern, Switzerland

*corresponding author: jasmine.berg@unil.ch

[a] Present address: School of Oceanography, Shanghai Jiao Tong University, Shanghai 200240, China

[b] Present address: Department of Ecology and Environmental Sciences, Umeå Universitet, 901 87 Umeå, Sweden

[c] Present address: Marine Science Institute, University of Texas at Austin, Port Aransas, TX 78373, USA

keywords: *sulfur cycling, sulfur isotopes, organic sulfur, early diagenesis, lake sediment, meromictic, Holocene, euxinic*

Field Code Changed

ABSTRACT

The sulfur cycle is very important in lake sediments, despite the much lower sulfate concentrations in freshwater than seawater. To date, little is known about the formation and preservation of organic and inorganic sulfur compounds in such sediments, especially in the sulfate-depleted subsurface. Here we investigated the fate of buried S-compounds down to 10-m sediment depth, which represents the entire ~13.5 kya sedimentary history, of the sulfate-rich alpine Lake Cadagno. Chemical profiles of sulfate and reduced sulfur reveal that sulfate from lake water is depleted at the sediment surface with the concomitant formation of iron sulfide minerals. An underlying aquifer provides a second source of sulfate and other oxidants to the deepest and oldest sediment layers generating an inverse redox gradient with ongoing sulfate consumption. ~~Active sulfur cycling within this deep layer produces highly~~The isotopic offsets between pools of humic acid-sulfur, acid-volatile sulfur (AVS) and ~~^{34}S-depleted~~ chromium-reducible sulfur (CRS)~~.~~, in both surface and deep sediments suggest differential timing of formation, with (~~δ^{34}S between -45 and -26 ‰ VCDT) and humic-bound sulfur compared to sulfate in lake (+24 ‰) or aquifer water (+12 to +15 ‰) or CRS in surface sediments (-12 to + 13 ‰). Overall, very similar $\varepsilon_{sulfate\ pyrite}$ isotope differences in both surface and deep sediments suggest rather comparable closed-system sulfur cycling despite the large differences in sulfate concentrations, organic matter content, and microbial community composition~~sulfide oxidation to sulfur/polysulfides playing an integral role in organic matter sulfurization. Although sulfate is depleted in the central part of the sediment column, *dsrB* gene libraries ~~suggest~~ reveal a potential for microbial sulfur reduction throughout the sediment column, with sequences in sulfate-depleted layers being dominated by Chloroflexota. Collectively, our data ~~suggest~~ indicate an active sulfur cycle that is driven by uncultivated microorganisms in deep sulfate-depleted sediments of Lake Cadagno.

Formatted: Not Highlight

Formatted: Not Highlight

46

1. INTRODUCTION

The biological sulfur cycle exerts an important control on organic matter burial and thus plays a major role in the global cycling of carbon, oxygen, nitrogen and iron. In anoxic marine sediments, microbial reduction of sulfate (SO_4^{2-}) to hydrogen sulfide (ΣH_2S) is quantitatively the most important respiration reaction, remineralizing upwards of 30% of the total organic carbon flux to the seafloor (Jørgensen, 1982; Bowles et al., 2014; Baloza et al., 2022). Even in freshwater systems, where sulfate concentrations are typically 100-1,000 times lower than in seawater, high rates of microbial sulfate reduction can be sustained by rapid reoxidation of ΣH_2S by Fe^{III}, Mn^{IV}, and possibly by redox-active organic substances, e.g. certain humic acids (Pester et al., 2012; Hansel et al., 2015).

Sulfur isotopic fractionation provides important insights into microbial sulfur cycling in the past and present by recording signatures of these processes within different sulfur pools, including sulfide minerals. The preferential reduction of ^{32}S- over ^{34}S-sulfate generates isotopic fractionations of 3 to 75 ‰ between sulfate and hydrogen sulfide in microbial cultures (e.g. (Kaplan and Rittenberg, 1964; Habicht and Canfield, 1997; Detmers et al., 2001; Rudnicki et al., 2001; Wortmann et al., 2001; Brunner and Bernasconi, 2005; Sim et al., 2011; Bradley et al., 2016)). Nonetheless, the dynamics and controls on the magnitude of sulfur isotope fractionation by sulfate reducing microorganisms have proven to be complex to understand in the environment. While pyrite $\delta^{34}S$ values supposedly record the S isotopic composition of sulfide in porewater fluids, major isotopic differences (between 10 and 40‰) have been observed between coexisting sedimentary pyrite and dissolved H_2S (Chanton et al., 1987; Canfield et al., 1992; Brüchert and Pratt, 1996; Raven et al., 2016; Lin et al., 2016). These discrepancies have been explained by processes such as sediment remobilization, bioturbation, or post-depositional sediment-fluid interactions (Jørgensen et al., 2004; Fike et al., 2015).

Formatted: English (United States)

Formatted: English (United States)

~~Recent work of Bryant et al. (2023) indicates~~While the δ^{34}S-composition of pyrite has been widely used to interpret global changes in the Earth's sulfur cycle or microbial metabolic pathways, an earlier body of work (e.g., Schwarcz and Burnie, 1973; Goldhaber and Kaplan, 1975, 1980; Maynard, 1980) showed that δ^{34}S-isotopic variations in marine sediments are largely controlled by local physical factors, such as sedimentation rate, along with the supply of Fe and OM~~(Bryant et al., 2023)~~. In open systems, the sulfate pool is constantly replenished with light ^{32}S-sulfate, whereas under conditions of rapid sedimentation, sulfate in sediment pore spaces is sealed off from overlying waters and the sulfate pool undergoes Rayleigh distillation (Hartmann and Nielsen, 2012). Closed versus open system sulfate reduction can thus explain the large variability in observed fractionations between sulfide and sulfate, which is recorded in sediments by authigenic pyrite (Bryant et al., 2023).

While pyrite is the dominant S pool in most marine sediments, the biggest S pool in many freshwater sediments is organic S (Mitchell et al., 1981; Nriagu and Soon, 1985; Losher, 1989; Urban et al., 1999). This organic S originates from both the settling of seston material and the microbial reduction of water column-derived sulfate to hydrogen sulfide, which then reacts with sedimentary organic matter (David and Mitchell, 1985; Rudd et al., 1986; Losher, 1989; Putschew et al., 1996; Damste et al., 1998). The sulfurization of organic matter tends to promote organic matter resistance to microbial degradation and is thus believed to contribute ~~significantly~~ substantially to long-term preservation of organic carbon in sediments (Damsté and De Leeuw, 1990; Hebting et al., 2006), and to petroleum formation (Orr and Damsté, 1990). Though it is likely that some microorganisms are capable of degrading fractions of this organic S pool, their activity and identity is unknown.

Recently, the metabolic capacity for sulfur cycling has been expanded to new phylogenetic groups based on the detection of specific marker genes for sulfur cycling within these taxa (e.g., Anantharaman et al., 2018). Although the presence of such genes must be

Formatted: English (United States)
Formatted: English (United States)
Formatted: English (United States)
Formatted: English (United States)
Formatted: English (United States)
Formatted: English (United States)

interpreted with caution, their distribution across environments can help illuminate the distributions of putative sulfur reducing and sulfur oxidizing microbial communities. Thiosulfohydrolase of the sulfur oxidation (Sox) enzyme system (*sox*B) is one such marker gene and has been widely employed to characterize the diversity of sulfur-oxidizing bacteria (SOB) (Meyer et al., 2007). Another example is dissimilatory sulfite reductase (*dsr*AB), an enzyme that catalyzes the reduction of sulfite to sulfide and is used by all known sulfate reducers (Klein et al., 2001).

Because low rates of microbial sulfur cycling continue in sulfate-depleted marine sediments (Holmkvist et al., 2011; Treude et al., 2014; Brunner et al., 2016; Pellerin et al., 2018a), such processes may likewise occur in sulfate-depleted sediments of lakes and leave a lasting imprint on the lake sulfur geochemical record. Here we investigate the potential for microbial sulfur cycling in Lake Cadagno, which is an intermediate system between freshwater and seawater, due to its elevated sulfate concentrations (1-2 mM). We combine chemical and isotopic analyses of major S and C phases with quantification and sequencing of S-cycling genes (*dsr*B, *sox*B) to investigate S cycling across the complete ~13.5 kya sedimentary history of Lake Cadagno.

METHODS

~~1.1~~ *2.1 Geological setting and sampling*

The meromictic Lake Cadagno, located in the Swiss Alps, contains 1-2 mM dissolved sulfate, which originates from the dissolution of sulfate-bearing dolomite bedrock via subaquatic springs. Since its formation ~13.5 kya, Lake Cadagno has undergone a complex redox history, transitioning from seasonal stratification around 12.5 kya to complete euxinia about 10.9 kya

Formatted: Font: (Default) Times New Roman, 12 pt, Bold, Italic, Font color: Black

Formatted: Normal, No bullets or numbering

(Wirth et al., 2013; Berg et al., 2022). Preliminary analyses of sulfur phases in surface and deep sediments (Berg et al., 2022) reveal two sulfate depletion zones (SDZ).

For high-resolution analyses, short cores were retrieved from the deepest part of the lake (46.55060 N and 8.71201 E) using a UWITEC gravity corer fitted with plastic liners with 1 m length and 9 cm inner diameter. Deep cores of 3-m long and 6-cm diameter core sections were recovered using a percussion piston-coring system (Uwitec, AT). More details are provided in (Berg et al., 2022). Cores from three parallel boreholes were reserved for non-destructive imaging, porewater extraction, and solid-phase analyses, respectively.

In brief, porewater was extracted using syringes connected to Rhizons (0.2 µm pore size, Rhizosphere) pre-flushed with 2–3 ml of pore water to remove contaminant air. Porewater was then distributed into separate vials with appropriate fixatives for downstream analyses described below. For solid-phase samples, windows were cut into the core liners using a hand-held vibrating saw and potentially contaminated sediment in contact with the liner was scraped away. Samples were then taken using sterile, cut-off syringes and frozen (-20°C) in separate aliquots for DNA and solid-phase extractions.

~~All Lake Cadagno deep sediment core sampling, geochemical analyses of sediment and porewater, and DNA extractions were performed as described in (Berg et al., 2022).~~ Additional samples for sulfate isotope analyses were obtained in June 2020 from one surface spring (at SwissGrid coordinates 2'697'763, 1'155'959) and one subaquatic spring at approximately 5 m depth (2'697'521, 1'156'044) located on the south side of the lake.

Porewater samples in 1991 were also collected from a gravity core from the deepest point in the lake. Porewater was extracted using a dialysis porewater sampler (Brandl and Hanselmann, 1991) consisting of 80 x 20 x 1.5 cm Plexiglas sheets containing 41 rows of cylindrical dialysis chambers, each 1.5 cm in diameter and 1.5 cm deep. The chambers were

Formatted: English (United States)
Formatted: English (United States)
Formatted: English (United States)
Formatted: English (United States)
Formatted: English (United States)
Formatted: English (United States)
Formatted: English (United States)
Formatted: English (United States)
Formatted: English (United States)
Formatted: English (United States)
Formatted: English (United States)
Formatted: English (United States)
Formatted: English (United States)
Formatted: English (United States)

covered on both sides with membranes held in place by 3 mm thick Plexiglas overlays. The membranes sealed the single chambers and prevented exchanges between them. Up to five individual samples of 2.6 mL can be collected from each row. Divers positioned the sampler in the sediment, leaving 10 cm extending above the sediment-water interface to collect bottom water samples, and it was allowed to incubate for two weeks. After recovery, the water of the individual chambers was immediately extracted from the chambers with a syringe and injected in a vial containing a silver nitrate solution to precipitate silver sulphide.

2.2 Porewater and solid-phase analyses

Samples for analysis of dissolved metals (Fe, Mn) were acidified with 5 µL of 30% HCl per 2 ml to prevent precipitation and measured by inductively coupled plasma optical emission spectroscopy (ICP-OES, Agilent Technologies 5100). Samples for dissolved sulfate analyses were immediately frozen at −20°C until analysis by ion chromatography (DX-ICS-1000, DIONEX)

The silver sulphide precipitate from 1991 porewater samples was recovered by centrifugation, dried and preserved for later sulphur isotope analysis. The remaining solution was acidified to pH<2 and sulfate was precipitated with $BaCl_2$, recovered by filtration and dried for analysis.

Total carbon (TC) and total sulfur (TS) were determined from oven-dried sediment (70°C) by EA-IRMS as described below. Total organic carbon (TOC) was determined after acid-extraction of inorganic carbon with concentrated 6 N HCl. Total inorganic carbon (TIC) was calculated as the difference between TC and TOC. Solid, reactive iron was determined on anoxically treated, freeze-dried samples by extraction with 0.25 mM HCl and subsequent photometric determination of Fe(II)/Fe(III) in the supernatant (Stookey, 1970).

Formatted: Font: Bold, Italic
Formatted: Font: Bold
Formatted: Font: Bold, Italic
Formatted: Font: Bold
Formatted: Font: Bold, Italic
Formatted: English (United States)
Formatted: English (United States)
Formatted: English (United States)
Formatted: English (United States)

2.3~~2~~ Solid-phase sulfur extractions

Sequential sulfur extractions were performed on freeze-dried samples based on the protocol of Ferdelman et al. (1991). First, elemental sulfur was extracted under N_2 atmosphere three times with degassed 100% methanol. During each step the methanol-sample mixture was sonicated for 10 min in an ice bath, centrifuged, and then the methanol was pipetted into a clean vial. Methanol extracts were analyzed by ultrahigh pressure liquid chromatography (UPLC) using a Waters Acquity H-class instrument with an Aquity UPLC BEH C18, 1.7 µm, 2.1 × 50 mm column (Waters, Japan) and a PDA detector (absorbance wavelength set to 265 nm). The injection volume was 10 µl with methanol as eluent flowing at 0.2 ml min^{-1}. Elemental sulfur eluted at 4.14 min.

Next, humic acids were extracted 3 times, or until the supernatant was clear, with degassed 0.1 M NaOH and collected in 50 ml Falcon tubes. Silicates were precipitated from the base extracts by addition of saturated NaCl solution (5 mL per 45 mL extract) and removed by centrifugation and decanting. The basic extract was acidified to pH 1.5 with concentrated HCl, allowed to stand at 4°C overnight, and centrifuged to precipitate humic acids. These were washed three times with distilled water to remove salts prior to drying and C, N, and S analysis.

Finally, acid-volatile sulfur (AVS) and chromium-reducible sulfur (CRS) were extracted from the remaining sediment using the two-step acid Cr-II method (Fossing and Jørgensen, 1989; Kallmeyer et al., 2004). For the AVS fraction, 6 N HCl was added to sediment in a reaction flask under an N_2 atmosphere and H_2S was trapped by bubbling through a 5% Zn-acetate solution for 2 h. The CRS fraction was subsequently obtained by adding 20 ml of the organic solvent dimethyl sulfoxide and 16 ml of $CrCl_2$ solution and reacting again for 2 h. AVS and CRS fractions, collected as ZnS, were quantified photometrically as above, pelleted by centrifugation, rinsed with MilliQ, and dried at 50°C prior to $\delta^{34}S$ analyses as described below.

2.4 Isotopic analyses

Isotopic compositions of sulfur in the sedimentary AVS, CRS and humic acid sulfur (HAS) fractions, and of dissolved sulfate from sediment porewater, a subaquatic spring, and two surface springs, were determined using a Flash-EA 1112 (ThermoFisher) coupled to an isotope ratio mass spectrometer (IRMS, Delta V, ThermoFisher) by addition of vanadium pentoxide as a catalyst. Isotope ratios are reported in the conventional δ-notation with respect to the Vienna-Cañon Diabolo Troilite (VCDT) standard for sulfur. The system was calibrated for sulfur using the international standards for sulfide and sulfate: IAEA-S1 ($\delta^{34}S$ = -0.3‰), IAEA-S2 ($\delta^{34}S$ = +22.67‰), IAEA-S3 ($\delta^{34}S$ = -32.55‰) and IAEA-SO5 ($\delta^{34}S$ = +0.49‰), IAEA-SO6 ($\delta^{34}S$ = -34.05‰), NBS-127 ($\delta^{34}S$ = +21.1‰), respectively. Reproducibility of the measurements was better than 0.2‰. This method also produced the weight % sulfur in the humic acid extracts.

The 1991 samples were measured at ETH Zürich by combusting 1-2 mg of silver sulphide sealed in Quartz glass tubes with copper oxide turnings at 950 °C. The SO_2 was separated from other combustion products using a pentane-liquid nitrogen slush and was measured on a VG 903 mass spectrometer. The system was calibrated with IAEA-S1 and IAEA-S3 and NBS 28. Reproducibility of the standards $\delta^{34}S$ value was better than ± 0.3 ‰.

~~Total sulfur (TS) was determined together with total carbon (TC) and total organic carbon (TOC) on bulk, freeze-dried sediments as described in (Berg et al., 2022) and TIC was calculated as the difference between TC and TOC.~~

2.5~~3~~ DNA extraction and sulfur-cycling gene analyses

Formatted: Font: Bold, Italic

Formatted: Indent: First line: 0 cm

Formatted: English (United Kingdom)

Formatted: Indent: First line: 0 cm

DNA was extracted from frozen sediment according to the lysis protocol II of (Lever et al., 2015) as outlined in (Berg et al., 2022). The *dsr*B gene was PCR-amplified using the *dsr*B F1a-h / 4RSI1a-f primer mixtures from (Lever et al., 2013). *sox*B genes were amplified using the recently designed *sox*B-837F1a-l / *sox*B_1170R1a-g primer mixtures (Deng et al., 2022). Quantitative PCRs (qPCR) were performed on a LightCycler 480 II system using the reagent mixtures outlined in (Jochum et al., 2017). The thermal cycler settings were (1) enzyme activation and initial denaturation at 95°C for 5 min; (2) 60 cycles of (a) denaturation at 95°C for 30 s, (b) annealing at 56°C (*dsr*B) or 60°C (*sox*B) for 30 s, (c) elongation at 72°C for 25 s, and (d) fluorescence acquisition at 82°C (*dsr*B) or 86°C (*sox*B) for 5 s; and (3) a stepwise melting curve from 60 to 95°C to check for primer specificity. Plasmids containing full-length *dsr*AB and *sox*B genes of *Desulfotomaculum carboxydivorans* and *Thiobacillus denitrificans*, respectively, were applied as qPCR standards.

*dsr*B gene sequences were phylogenetically annotated using the ARB software (www.arb-home.net) based on an updated version of the *dsr*AB database published in (Müller et al., 2015). This database was expanded by adding *dsr*AB gene sequences from since then published metagenomes, as well as closest BLAST hit to *dsr*B gene sequences detected in Lake Cadagno. The phylogenetic annotation was based on a *dsr*AB gene bootstrap tree that was built by ARB Neighbor-Joining with Jukes-Cantor correction using diverse *dsr*AB reads that covered the entire *dsr*B gene amplicon sequence and were at least 750 bp in length. The shorter amplicon sequences from Lake Cadagno, as well as closest BLAST hits that were <750 bp long, were added using the ARB Parsimony option combined with a newly designed, amplicon-specific *dsr*B filter that removed hypervariable regions.

~~2.~~ 3. RESULTS

~~2.1~~ *3.1 Sulfur Geochemistry in Lake Cadagno sediments*

Formatted: Font: (Default) Times New Roman, 12 pt, Bold

Formatted: Normal, No bullets or numbering

Formatted: English (United States)

Formatted: Font: (Default) Times New Roman, 12 pt, Bold, Italic, English (United States)

The complete sedimentary sequence from Lake Cadagno is approximately 950 cm long, covering a period of ~13.5 ky (Berg et al., 2022). Sediments are characterized by relatively fine grained pelagic lacustrine sediments intercalated with frequent coarser-grained flood- and mass movement-derived deposits containing remobilized littoral lake and terrestrial sediment in the upper 790 cm, underlain by light-colored fine-grained deposits of late glacial origin (Fig. 1). The sediment can thus be divided into three distinct lithostratigraphic units representing an early oxic lake (950-790 cm; 13.5 to 12.5 kya), a redox transition interval (790-760 cm; 12.5 to 10.9 kya), and the euxinic period (above 760 cm; 10.9 kya to present). High-resolution mapping of element geochemistry on split core surfaces (Fig. 1) reveals that the accumulation of sulfur is restricted to sediments deposited after the onset of periodic anoxia (transition interval) to permanently reducing conditions (euxinic interval). Fe and S were normalized against Ti, which represents the lithogenic fraction unaltered by redox processes in the aquatic environment. The correlation between S/Ti and Fe/Ti suggests the presence of authigenic iron sulfide phases. The

largest S excursions are located at 300, 560, and 637, which correspond to lacustrine deposits according to the lithological sequence.

Figure 1| Lithological profile determined from a composite core image of the sedimentary sequence retrieved from Lake Cadagno. XRF profiles of S/Ti and Fe/Ti from Berg et al (2022). Changes in lake redox chemistry are denoted by dashed lines.

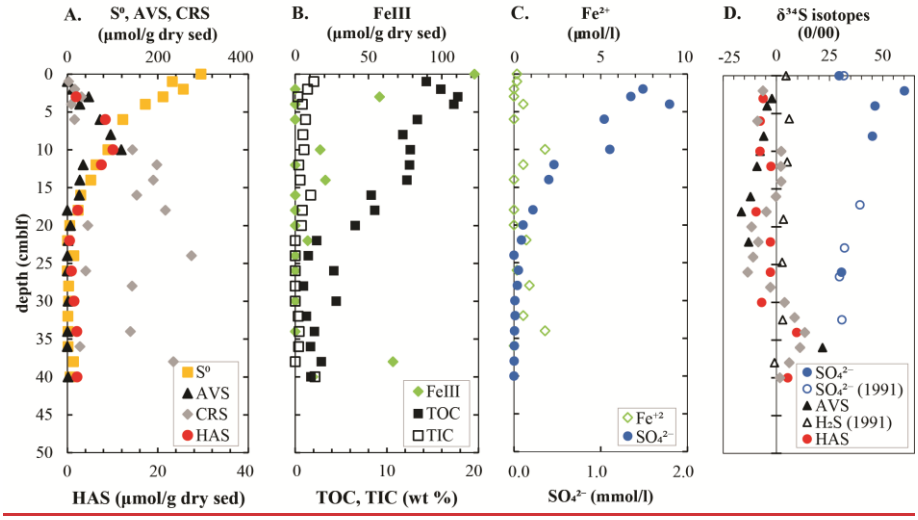

Figure 2| Geochemistry of (A) major solid-phase sulfur pools ~~(A)~~ along with (B) ~~metals~~ FeIII and ~~dissolved species~~total organic and inorganic carbon ~~(B)~~ and (C) dissolved species involved in sulfur cycling in the ~~sediment column~~ surface sediments of Lake Cadagno. ~~(C) Ratios of total and organic~~

To obtain further insights into sulfur redox cycling in these sediments, major solid sulfur phases were quantified (Fig. 2A). Elemental sulfur (S^0) is the most abundant solid sulfur phase in surface sediments at 300 µmol/g dry sediment. The parallel decrease in S^0 and Fe^{III} (Fig. 2B) with depth indicate increasingly reducing conditions. Both AVS (mostly amorphous FeS and mackinawite) and HAS exhibit a peak at 10 cm depth, which coincides with a peak in dissolved Fe^{2+} and the steepest decrease in sulfate concentrations (Fig. 2C). Below this depth, AVS, HAS, and S^0 ~~and then~~ decrease in parallel with ~~S^0~~ sulfate at the expense of CRS formation. Most carbon is in organic form in the Lake Cadagno sediments, with measurable contributions (<2

Figure 2| Geochemistry of (A) major solid-phase sulfur pools ~~(A)~~ along with (B) ~~metals~~ FeIII and ~~dissolved species~~total organic and inorganic carbon ~~(B)~~ and (C) dissolved species involved in sulfur cycling in the ~~sediment column~~ surface sediments of Lake Cadagno. ~~(C) Ratios of total and organic carbon to sulfur and humic acid bound S, respectively, along with~~ (D) ~~isotope~~ Isotope ratios of major sulfur pools with data from 1991 represented as open symbols overlain on profiles from 2019.

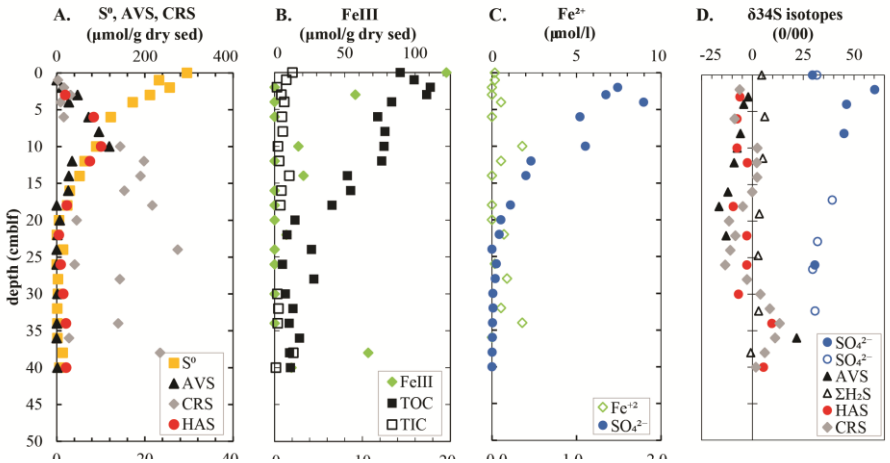

wt%) of total inorganic carbon (TIC) present only in the top few centimeters and again at 14 cm depth (Fig. 2B).

Notably, $\delta^{34}S$ isotope $\delta^{34}S$ sulfate profiles measured more than 30 years apart coincide surprisingly well (Fig. 2D). Sulfate in the upper sediments is highly enriched in ^{34}S, increasing from +24 ‰ in the bottom waters to +60 ‰ within the upper 2 cm. This zone coincides with strong decreases in TOC and isotopically light ^{13}C-DIC values, which indicate high rates of organic matter mineralization (Berg et al., 2022; Gajendra et al., 2023). ~~$\delta^{34}S$ sulfate profiles measured in 1991 exhibit increasing enrichment in ^{34}S down to the SDZ (Fig. S2) with the highest values of approximately 60‰ at 10 cm depth, somewhat deeper than at present.~~There is a small but consistent offset between $\delta^{34}S$ in reduced sulfur pools of H_2S, AVS, HAS and CRS but no real trends. The widest fluctuations of $\delta^{34}S$ values were measured in the AVS with -16 ‰ at +16 cm and 22‰ at 34 cm depth.

Formatted: Not Highlight

Formatted: Font: Not Bold

In mid-column sediments~~sediments below~~ between ~~2~~150 and 760 cm, S^0 and AVS are barely or not detectable whereas HAS concentrations are relatively constant (0.42 - 4.40 µmol/g dry sed) and CRS levels fluctuate widely (0-270 µmol/g dry sed). The highest concentrations of CRS and HAS are associated with lacustrine deposits (Fig. 3A). In the deep euxinic sediments, exceptionally high CRS contents were detected in a handful of samples that are typically lacustrine deposits and follow broadly the same trend as solid FeIII and dissolved Fe^{2+} concentrations (Fig. ~~2B~~3B,C).

At 760 cm, a second SDZ has been described based on an upwards-diffusing gradient of sulfate thought to originate from a subterranean aquifer (Berg et al., 2022). The change in redox conditions at 775 cm depth is marked by a small peak in AVS (9 µmol/g dry sed) and S^0 (23 µmol/g dry sed). In concurrence with extant oxidizing conditions, late glacial sediments

Figure ~~2~~3 | Geochemistry of (A) major solid-phase sulfur pools ~~(A)~~ along with (B) ~~metals~~ FeIII and ~~dissolved species~~total organic and inorganic carbon ~~(B)~~ and (C) dissolved species involved in sulfur cycling in the ~~sediment column~~ deep sediments of Lake Cadagno. ~~(C) Ratios of total and organic carbon to sulfur and humic acid bound S, respectively, along with~~ (D) ~~isotope~~ Isotope ratios of major sulfur pools. Note that sufficient porewater was obtained to measure sulfate isotopes by pooling five deep sediment samples and are thus an average value. ~~Based on previous analyses (Berg et al 2022), the sulfate depletion zones have been shaded in gray and lacustrine deposits have been shaded in blue. Note the break in the y-axis.~~

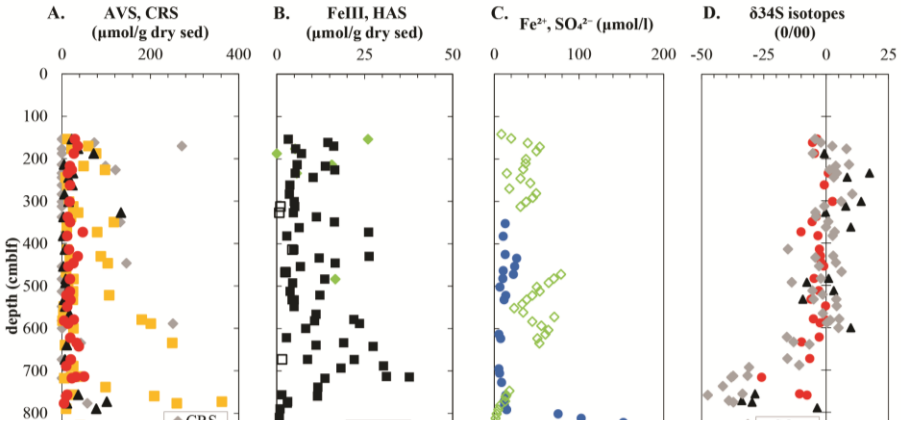

Formatted: Not Highlight
Formatted: Not Highlight
Formatted: Not Highlight
Formatted: Not Highlight
Formatted: Not Highlight
Formatted: Not Highlight
Formatted: Not Highlight
Formatted: Not Highlight
Formatted: Not Highlight

below 790 cm are poor in reduced sulfur and organic matter but contain measurable iron oxides and up to 0.2 mmol/l sulfate in porewaters (Fig. ~~2B~~3B,C). These sulfate concentrations are much lower than concentrations of sulfate in lake bottom water (1.8 mmol/l), but in the same general range as a subaquatic spring (0.~~268~~27 ~~µmol~~mmol/l) and a surface spring (~~166~~ 0.17 ~~µmol~~mmol/l).

~~C to S ratios of organic matter are expected to decrease when sulfide reacts with organic matter to form organic S, or when microorganisms preferentially degrade organic carbon and leave behind organic S. TC:TS decreases from 12 at the surface to about 1.3 at 20 cm depth and remains relatively constant throughout the deeper sediments (Fig. 2C). Most of this carbon is in organic form, with measurable contributions of total inorganic carbon (TIC) present only in surface sediment and again at 400 cm depth (<2 wt%; Fig. S1). A part of the total organic sulfur could be measured as HAS, and the ratios of TOC:HAS exhibit a very different behavior (Fig. 2C). TOC:HAS was lowest at 25-40 cm depth and the rather high, widely fluctuating values below this depth are mostly due to the low TOC content.~~

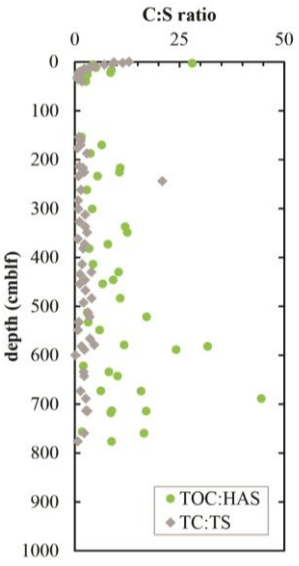

Figure ~~2~~4| ~~Geochemistry of major solid-phase sulfur pools (A) along with metals and dissolved species (B)~~

Sufficient sulfate for isotopic analyses ~~was~~ could only be ~~only~~ obtained ~~from five surface samples and~~ by pooling porewater from the entire late glacial sediment sequence (790-910 cm). ~~Sulfate in the upper sediments is highly enriched in ^{34}S, increasing from 24 ‰ in the bottom waters to 60 ‰ within the upper 2 cm. This zone coincides with strong decreases in TOC and isotopically light ^{13}C-DIC values, which indicate high rates of organic matter mineralization (Berg et al., 2022; Gajendra et al., 2023). $\delta^{34}S$-~~

~~sulfate profiles measured in 1991 exhibit increasing enrichment in ^{34}S down to the SDZ (Fig. S2) with the highest values of approximately 60‰ at 10 cm depth, somewhat deeper than at present.~~ In the deep glacial sediments, ~~the~~ this averaged sulfate isotopic signature is relatively light (+7‰), which is more similar to values measured in subaquatic (+12‰) and surface (+15‰) springs (Fig. 3D). Isotopic values of reduced sulfur pools fluctuate between positive and negative values

~~Sulfide in Lake Cadagno sediments is generally depleted in ^{34}S relative to sulfate in the overlying water column (Fig. S2). δ^{34}S-AVS becomes progressively lighter with depth in surface sediments, decreasing from ~2‰ at the lake floor to a minimum value of ~16‰ in the upper SDZ, but very little AVS was recovered from the mid-column and deep sediments. For those samples with measureable δ^{34}S-AVS, it fluctuates between ~9‰ and +17‰~~ with no discernible trend. In the deep SDZ, δ^{34}S-AVS becomes strongly negative, exhibiting values as low as -34‰ coinciding with lighter porewater sulfate (+6.8‰). CRS is more depleted in ^{34}S than AVS ~~in the limited samples available, except for in the upper SDZ where δ^{34}S-CRS values are enriched by ~2‰ relative to δ^{34}S-AVS. I~~in ~~the deep SDZ~~this zone, with extremely light ~~CRS~~ values ~~are observed down to~~of -47.5‰ at 760 cm~~,~~ which is equivalent to a fractionation of 54‰ compared to deep porewater sulfate. δ^{34}S-HAS are consistently ~~heavier~~ less negative than AVS and CRS, varying between 0‰ and -26‰ down to 750 cm depth in respective sediment layers. ~~-~~No significant difference in HAS isotopic composition was found between sediment layer types.

C to S ratios of organic matter are expected to decrease when sulfide reacts with organic matter to form organic S, or when microorganisms preferentially degrade organic carbon and leave behind organic S. TC:TS decreases from 12 at the surface to about 1.3 at 20 cm depth and remains relatively constant throughout the deeper sediments (Fig. 4). Most of this carbon is in organic form, with measurable contributions of total inorganic carbon (TIC) present only in

surface sediment and again at 400 cm depth (<2 wt%; Fig. 2B). The apparent outlier at 243 cm is due to very low sulfur concentrations measured in this sample. A part of the total organic sulfur could be measured as HAS, and the ratios of TOC:HAS exhibit decrease from the surface to 25 cm depth (Fig. 4). Below 150 cm depth, ratios of TOC:HAS fluctuate widely, following the same trend as TOC.

Formatted: Do not check spelling or grammar

3.2 Genetic potential for microbial sulfur cycling

Abundances of sulfur-cycling microorganisms in the Lake Cadagno sediment column were assessed by qPCR of functional genes for sulfate reduction (*dsr*B) and sulfur oxidation (*sox*B) (Fig. ~~3~~5). Copy numbers of *dsr*B gradually decrease from surface sediments (4.23 x 10^8 copies/g wet sediment) to the upper SDZ (7.17 x 10^6 copies/g, 44 cm depth). Throughout the SDZ (35 cm and below), gene copy numbers remain relatively stable between 1.58 x 10^6 and 2.9 x 10^7 copies/g wet sediment. Within the lower sulfate-methane depletion zone at around 810 cm depth, *dsr*B copy numbers drop off greatly, to values of 10^1 and 3.10 x 10^3 and copies/g before increasing again to 2.77 x 10^4 copies/g in parallel with increasing sulfate concentrations in the underlying oxic, glacial interval (Fig. ~~3~~5; also see Fig. ~~1~~2C).

Figure ~~3~~5 Depth profiles of *dsr*B and *sox*B gene copy numbers. Copies of both genes were detectable by qPCR in all samples targeted. Shaded gray regions indicate sulfate-methane depletion zones.

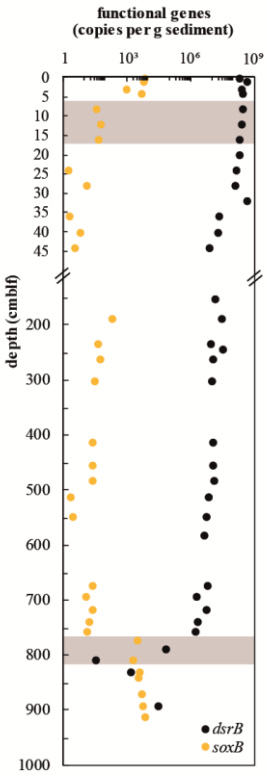

Surprisingly, *sox*B was detectable throughout the entire sediment column. Highest values (up to 6.45 x 10^3 copies/g sediment) were found in the sulfate-rich surface sediments down to the SDZ. In mid-column sediments, sulfur oxidation gene copies were much lower (1.84 x 10^0 -1.93 x 10^2 copies/g) before increasing again in the lower SDZ and reaching a second peak in the glacial sediment layer (6.59 x 10^3 copies/g). This increase in sulfur oxidation potential matches the oxidizing, and most likely oxic, conditions in this deep glacial sediment layer that are by the presence of Fe-oxides, elemental sulfur, and sulfate (Fig. ~~2A~~3A~~&B~~ C). Sulfur oxidizing bacteria appear to make up a large part of the total microbial population in this layer, with an average ratio of *sox*B to 16S DNA copies/g sediment of 1.17 ± 1.34. At the same time, 16S qPCR data indicate a drop in microbial population size from 10^8 copies/g sediment in the lower SDZ to 10^3 to 10^5 copies/g in the deep glacial layer (Berg et al., 2022).

Figure ~~3~~5 Depth profiles of *dsr*B and *sox*B gene copy numbers. Copies of both genes were detectable by qPCR in all samples targeted. Shaded gray regions indicate sulfate-methane depletion zones.

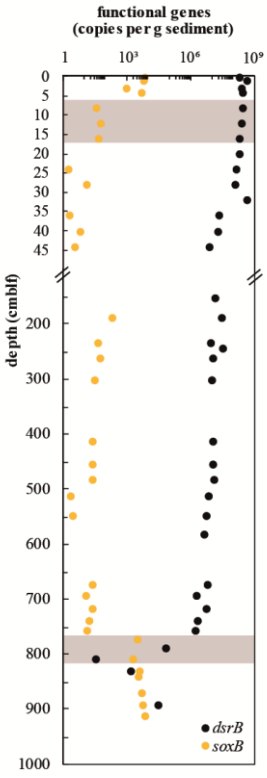

3.3 Diversity of sulfate-reducing microorganisms

Sequencing of the sulfate reduction gene (*dsr*B) revealed a diverse assembly of potential sulfate reducers in Lake Cadagno sediments (Fig. ~~4~~6). The majority of sequences could not be classified beyond the supergroup level, indicating that they belong to novel lineages. Overall, the sulfate reducers identified in our gene amplicon libraries were consistent with those identified in 16S rRNA gene libraries, with high relative abundances of Deltaproteobacteria, Nitrospirae, and Chloroflexota (Berg et al., 2022). The community profile shows a clear

differentiation between surface sediment and deeper sulfate-depleted layers, and there is a clear decrease in taxonomic diversity with depth and sediment age.

Similar to other sulfate-rich sedimentary environments, Lake Cadagno surface sediments harbor highly abundant (>80% relative abundance) Desulfobacterota (formerly

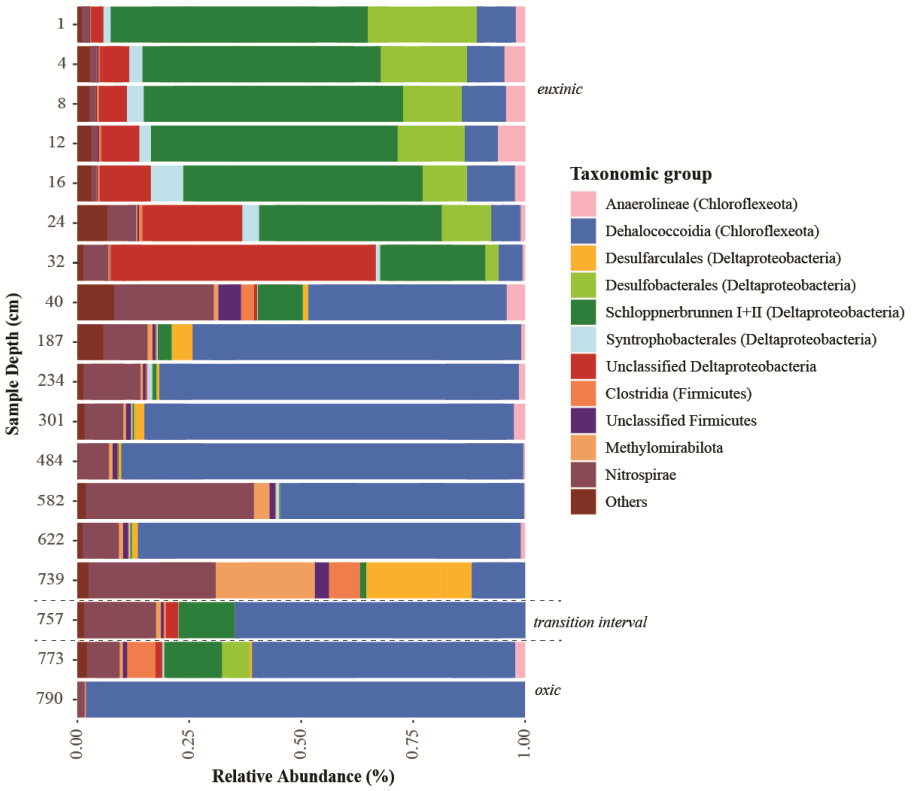

Figure 46 Taxonomic classification of functional genes *dsrB* recovered from the Lake Cadagno sediment depth. Sediment geological transitions are indicated with dashed lines.

Deltaproteobacteria). Most of these belong to uncultured members of the order Desulfobacterales, clade Schlöppnerbrunnen I + II (originally identified in peatland soils), and other unclassified Deltaproteobacteria. In addition, reads belonging to the genus *Desulfomonile*, of which members are known to also disproportionate sulfur intermediates (Slobodkin and

Slobodkina, 2019), are well represented in sediments between 4 cm and 28 cm below the sediment surface (2%-8% of the total community).

Below the SDZ at 40 cm there is a shift in the sulfate-reducing microbial assemblage toward the dominance of uncultivated Chloroflexota. Members of this phylum have so far not been demonstrated to perform dissimilatory sulfur cycling but Chloroflexota *dsrB* sequences have been found in deep sedimentary marine environments (e.g. Vuillemin et al., 2020; Liu et al., 2022). A second compositional shift occurs in deeper layers around the redox transition interval at 739 cm depth. Genes for sulfate reduction in these layers affiliate with Clostridiales, Dehalococcoidia, Methylomirabilales, and the phylum Nitrospirae. Sulfate reducers belonging to Desulfobacterota also reappear close to the redox transition but are distinct from those in surface sediments, affiliating mostly with the species *Desulfoarculus baarsii* (classified within the order Desulfarculales). In the deep glacial sediment (> 790 cm), the diversity of microbial sulfate-reducers is reduced (98% of *dsr*B sequence reads) to Chloroflexota from the classes Anaerolineae and Dehalococcoidia.

~~3.~~4. DISCUSSION

4.1 Evidence for continued sulfur cycling in sulfate-depleted sediments

The relatively heavy isotopic signature of sulfate in Lake Cadagno bottom waters ($\delta^{34}S$ = +24 ‰) compared to the $\delta^{34}S$ of source waters observed in subaquatic +12‰ and surface springs +15‰ indicate active sulfate reduction in the anoxic lower part of the water column. These values are consistent with previously measured values of surface (+12‰) and bottom water (+30‰) sulfate (Canfield et al., 2010). The $\delta^{34}S$ values of sulfate in the Lake Cadagno springs are the same as those of other springs in the Valle Leventina (Steingruber et al., 2020) indicating dissolution of gypsum/dolomite in the marine evaporites from the Middle Triassic ($\delta^{34}S$ circa +15‰) as the main source (Bernasconi et al., 2017).

Formatted: Font: (Default) Times New Roman, 12 pt, Bold

Formatted: Numbered + Level: 1 + Numbering Style: 1, 2, 3, … + Start at: 4 + Alignment: Left + Aligned at: 0 cm + Indent at: 0,63 cm

Microbial sulfur cycling in the sulfate-rich uppermost sediment layer (0-24 cm) appears to be primarily driven by Desulfobacterota. Below this depth, mostly uncultured groups of unclassified Deltaproteobacteria and Dehalococcoida possess an unexplored genetic potential for sulfate reduction. The high input of labile, microbial organic carbon from the overlying water column supports very high rates of anaerobic organic carbon mineralization within the upper 20 cm (Gajendra et al., 2023). As a result, TOC drops from 15-20 wt. % at the lake floor to values of ≤5 wt. % below 20 cm. Microbial sulfate reduction appears to be primarily linked to the degradation of this organic matter (Berg et al., 2022) though sulfate-driven AOM may additionally occur within the top 2-3 cm (Schubert et al., 2011). Vertical shifts in dominant S-cycling microorganisms from surface sediments (Schloppnerbrunnen I + II, Desulfobacterales (all Desulfobacterota) to Unclassified Desulfobacterota in deeper layers suggest a key influence of sulfate concentrations and organic matter quality on sulfate-reducing microbial community structure. Herein Desulfobacterales include several known sulfate-reducing and sulfur-disproportionating genera, such as *Desulfobulbus*, *Desulfovibrio*, and *Desulfomonile* (Cypionka et al., 1998; Wasmund et al., 2017; Hashimoto et al., 2022). Similar shifts in dominant sulfate-reducing communities from significant abundances of known groups with cultured representatives in surface layers to dominance of physiologically unclassified taxa in deeper layers have been reported from marine sediments (Jochum et al., 2017). We also detected genes for sulfur oxidation, despite the anoxic nature of these sediments~~.~~, possibly belonging to the aerobe *Sulfuricurvum* previously identified in surface sediments (Berg et al., 2022). It is presumed that bottom waters are anoxic, but sufficient iron oxides (and likely manganese oxides) are available to drive reoxidation of sulfide to elemental sulfur (Fig. 2A,B).

As sulfate concentrations drop below detection below 30 cm depth, there is a clear shift in dominance from Desulfobacterota to Chloroflexota (Fig. ~~4~~6). Nevertheless, *dsr*B gene abundances remain high suggesting that sulfate/sulfur reduction likely continues in sulfate-

Formatted: Font: Italic

Formatted: Font: Italic

Formatted: English (United States)

depleted sediments parallel to fermentation and methanogenic metabolisms. It is possible that sulfate or other oxidized sulfur species, that are regenerated by sulfur oxidation reactions with metal oxides, support these communities of S-cycling microorganisms. Alternatively, the high abundances of Chloroflexota from the class Dehalococcoidia could suggest alternative sulfur-based metabolic activities. Several studies have proposed Chloroflexota to be involved in the metabolism of organic sulfur compounds (Wasmund et al., 2014; Mehrshad et al., 2018), with genomic analyses from deep sea sediments indicating genetic potential for dimethylsulfide, methane sulfonate, and alkane sulfonate metabolisms (Liu et al., 2022). Overall, our findings are consistent with studies of marine sediments demonstrating active sulfate reduction below the zone of sulfate depletion (Holmkvist et al., 2011; Treude et al., 2014; Brunner et al., 2016; Pellerin et al., 2018b) and suggest that deep sulfate reduction also can occur in lake sediments.

An oxidizing front and constant groundwater supply of sulfate at the transition between euxinic and deep glacial deposits appears to sustain continuous microbial sulfur cycling at 760-800 cm depth. Opposite trends of *dsr*B and *sox*B gene copies reveal a physical separation between S reduction and oxidation in this layer indicating a switch from anoxic to oxic conditions. ~~δ^{34}S of CRS values that are depleted by ~40 and ~50 ‰ relative to those of δ^{34}S-sulfate suggest the presence of an active sulfur cycle driven by slow diffusion of groundwater sulfate into the deepest layers of lake sediment. Extremely slow sulfate reduction rates tend to generate very light sulfide, especially in a diffusive rather than closed system (Goldhaber and Kaplan, 1980; Habicht and Canfield, 1997; Ono et al., 2014), which is then preserved in the CRS pool over geological time scales. It can also not be ruled out that these low δ^{34}S values are due to repeated cycles of reduction and partial re-oxidation of H_2S, e.g. by chemical oxidation to S^0 by iron oxides followed by microbial S disproportionation (Canfield and Thamdrup, 1994) and/or by sulfur reduction (Wortmann et al., 2001; Brunner and Bernasconi, 2005b; Canfield et al., 2010; Sim et al., 2011). Single-step reduction of light S^0 appears to be the more~~

~~parsimonious scenario as the disproportionation model requires heavy sulfate to be removed from the system to avoid producing heavy sulfide. Nonetheless, iron oxides in the deep glacial layers are likely to oxidize (downward-diffusing) H_2S and may explain the abundant elemental S^0 measured at the deep redox transition.~~

4.2 Rapid degradation and sulfurization are controlled by organic matter quality

Major changes in solid-phase sulfur pools occur within the upper 20 cm of sediment corresponding to the very high rates of organic matter degradation and microbial sulfate reduction (Berg et al., 2022), These changes include a shift from elemental S and AVS as the dominant S pools at 0-10 cm to CRS (which contains pyrite) as the main S pool between 10-20 cm. This CRS likely derives from chemical reactions of AVS (containing FeS) and elemental sulfur (including polysulfides) (Luther, 1991). Below 20 cm, CRS remains the dominant S pool, and moreover, shows a highly significant ($p < 0.001$) enrichment in lacustrine layers versus mass-movement deposits. The elevated CRS in lacustrine layers confirms the notion that most iron sulfides are of authigenic (rather than terrestrial) origin and result from anaerobic breakdown of lacustrine organic matter driving sulfate reduction.

In addition to CRS formation, we observe the sulfurization of organic matter in these (<100-year-old) surface sediments, as indicated by the strong increase in HAS (up to 10 µmol/g sed) in the top 0-10 cm along with a drop in TOC:HAS ratios (Fig. 4). This observation is consistent with studies on several other lakes in Switzerland, which reported that most organic matter sulfurization occurs within the initial decades after sediment deposition (Urban et al., 1999; Hebting et al., 2006). Although humic acids are known to be persistent in ancient sediments~~(Brüchert, 1998)~~, a fraction of the HAS appears to be lost at 10-15 cm depth. It has been shown that sulfide released from fulvic acids contributes to ^{34}S-enriched CRS (Brüchert, 1998), and a similar release of sulfide from HAS depth could be the cause of more positive $\delta^{34}S$

Formatted: Indent: First line: 1,25 cm

Formatted: English (United States)

Formatted: English (United States)

Formatted: Superscript

CRS in our profiles becomes despite a concurrent depletion in ^{34}S-sulfate 10-15 cm below the lake floor.

It is also possible that variations in HAS concentrations are simply due to sediment origin. ~~Notably, the highest concentrations of~~Lacustrine sediment enriched in HAS is interspersed with HAS-poor m~~were recovered from lacustrine layers.~~ass movement deposits containing predominantly terrestrial material beginning at 18-22 cm depth and also forming thicker deposits such as from 31-55 cm depth (Fig. 1).

~~The observed high rates of organic matter sulfurization in surface sediments suggest that differences in organic matter quality affect organic matter degradation rates and may also affect the incorporation of sulfur into organic matter. Notably, the highest concentrations of HAS were recovered from lacustrine layers.~~ This suggests that fresh lacustrine organic matter from the lake water column is more easily sulfurized than refractory terrestrial organic matter from the lake watershed. While the chemical composition of this sulfurized organic matter remain unclear, it is worth noting that lipid-rich algal and microbial material are rapidly degraded in surface sediments, carbohydrates appear to be selectively preserved, thus increasing in contribution to total organic matter in deeper layers (Gajendra et al., 2023). This effective preservation of carbohydrates could be related to macromolecular matrices that are rich in degradation-resistant structural polymers (e.g. hemicelluloses and pectin in microalgal and terrestrial plant biomass; (Gajendra et al., 2023)). In addition, the high chemical reactivity of carbohydrates with sulfide could play a role. Past research has shown that carbonyl functional groups are more reactive with inorganic sulfur species than hydroxyl groups, explaining why carbohydrates with a carbonyl group in the C_1 position constitute a major part of sulfurized organic matter in marine sediments (Damsté et al., 1998) and in laboratory experiments (Kok et al., 2000). The same could be the case, leading to the effective preservation of carbohydrates in deeper sediment layers of Lake Cadagno ~~to be effectively preserved~~ because of sulfurization.

Alternatively, it is possible that sulfur ~~that is~~ incorporated into carbohydrates is selectively preserved as organic S because the surrounding carbohydrate matrices are ~~degradation-resistant~~degradation resistant.

Deeply buried organic sulfur in Lake Cadagno is more enriched in $\delta^{34}S$ than co-occurring pyrite which is consistent with measurements from marine systems (Goldhaber and Kaplan, 1980; Anderson and Pratt, 1995; Brüchert, 1998; Werne et al., 2003; Raven et al., 2016, 2023). ~~Humic sulfur consists of sulfoxides or sulfones and, in a more reduced state, o~~Organic sulfides ~~and/or organic polysulfides~~ or thiols are the major forms of reduced sulfur in humic acids (Ferdelman et al., 1991; Brüchert, 1998; Urban et al., 1999). ~~These distinct classes of organic S compounds exhibit different ^{34}S isotope signatures (Raven et al., 2015), and may have different source molecules (e.g., sulfate esters) than sulfur that is present in pyrite (e.g., inorganic sulfate)(Huc and Durand, 1977).~~ Because the fractionation factor of organic matter sulfurization is almost negligible (Amrani and Aizenshtat, 2004), it is likely that the timing of formation is responsible for HAS being heavier, on average, than CRS. Sulfur in HAS is derived from ^{34}S-enriched polysulfides produced by sulfide oxidation (Putschew et al., 1996; Brüchert, 1998; Werne et al., 2008), ~~which forms first and leaves behind a slightly heavier pool of sulfate/sulfide. Another explanation is that HAS~~This HAS is very stable (Brüchert, 1998) and less likely to be re-oxidized and undergo additional fractionation cycles. ~~(Brüchert, 1998)~~

While humic acid comprises only a small part of total organic sulfur in some sediments, it is highly persistent and a major component of total buried organic carbon (Huc and Durand, 1977). Here we estimate that an average of 2.6 ± 3.2 % of total organic carbon was extracted as HA. Because timing of formation appears to govern ^{34}S isotope signatures of the reduced sulfur pools, we also expect that progressive organic matter (i.e., carbohydrates and lipids) sulfurization results in compounds of increasing molecular weight such as S-containing

Field Code Changed

Formatted: Not Highlight
Formatted: Not Highlight
Formatted: English (United States), Not Highlight
Formatted: Not Highlight
Formatted: English (United States), Not Highlight
Formatted: Not Highlight
Formatted: Not Highlight
Formatted: Not Highlight
Formatted: Not Highlight
Formatted: Not Highlight
Formatted: Not Highlight
Formatted: English (United States)

kerogens (Sinninghe Damsté et al., 1990; Eglinton et al., 1994) enriched in ^{34}S~~(Sinninghe Damsté et al., 1990; Eglinton et al., 1994)~~.

Formatted: Superscript

4.3 ~~Diffusive dominated s~~Cycles of sulfate reduction and sulfide oxidation drive isotope fractionation in both ~~both~~ surface and deep sediments

Rayleigh distillation exerts a strong control on δ^{34}S signatures in sediments where diffusion limitations imply that sulfate cannot be replenished as rapidly as it is removed by microbial reduction and precipitation. For this reason, it has been postulated that at high rates of sedimentation, porewater sulfate is effectively trapped and the system closed off from exchange with the overlying water column (Bryant et al., 2023). The opposite is true for diffusive systems, where a constant supply of sulfate can feed continued production of light sulfide. In Lake Cadagno surface sediments (above the first mass movement deposit at 30 cm), the relatively large differences (44 to 66 ‰) in δ^{34}S between sulfate and CRS are in the same range as those previously measured in sediment incubations (Canfield et al., 2010). Interestingly, δ^{34}S sulfate profiles measured more than 30 years apart coincide surprisingly well, with sulfate becoming progressively heavier with depth (Fig. 2D) as is typical of closed system sulfate reduction. ~~In Lake Cadagno surface sediments (above the first mass movement deposit at 30 cm), the relatively large differences (44 to 66 ‰) in δ^{34}S between sulfate and CRS are in the same range as those previously measured between sulfate and sulfide in the porewaters in 1991 (Fig. S2) and in sediment incubations (Canfield et al., 2010). It is most evident from the oldest profile (Fig. S2) that δ^{34}S sulfate and CRS values become progressively heavier with depth across the top 20 cm typical of a closed system sulfate reduction.~~ In fact, sedimentation rates of 2-4 mm/yr have been reported for Lake Cadagno (Birch et al., 1996) which are rather high for a lake (Fiskal et al., 2019).

~~Although~~ Pools of reduced sulfur ~~CRS is~~ are on average more depleted in $\delta^{34}S$ in the deep glacial sediments than in surface sediments, ~~,~~ but the differences between porewater sulfate and ~~CRS~~ HAS ($\varepsilon_{sulfate\text{-}HAS}$ =14-32 ‰), AVS ($\varepsilon_{sulfate\text{-}AVS}$ = 9-45 ‰), and CRS ($\varepsilon_{sulfate\text{-}CRS}$ = 36-53 ‰) ~~is~~ are ~~around~~ actually smaller ~~the same as in surface sediments (45.8‰)~~. Nonetheless, the values should be taken with caution as a single value of $\delta^{34}S$-sulfate (+7 ‰) was successfully measured below 760 cm and thus represents an average of $\delta^{34}S$-sulfate in the deep glacial sediments. The relatively light pool of sulfate could result from oxidation of buried AVS and CRS by a groundwater source of oxidants mixing with groundwater sulfate (+12 ‰). This is supported by an increase in *sox*B gene copies (Fig. 5), along with the presence of abundant elemental S^0 (Fig. 3A) at the deep redox transition. Light sulfate is likely the main determinant of the highly negative $\delta^{34}S$ values of reduced sulfur.

All three reduced sulfur pools become progressively depleted in $\delta^{34}S$ moving downward through the sediment column towards the groundwater source. This is clear evidence of ongoing sulfate reduction, though the very low organic carbon content (0.2-0.3 wt %) suggests that rates are very slow and may be coupled to H_2 or methane oxidation. Extremely slow sulfate reduction rates can contribute to the production of very light sulfide, especially in a diffusive rather than closed system (Goldhaber and Kaplan, 1980; Habicht and Canfield, 1997; Ono et al., 2014).

~~An gradient of progressively heavier CRS can be observed moving upward through the sediment column away from the groundwater source. This suggests that closed-system sulfate reduction is leading to similar $\delta^{34}S$ fractionations as in surface sediments. What explains the rather light sulfate (+6.8 ‰) present in this deep layer remains unclear, but oxidation of buried CRS by a groundwater source of oxidants offers a potential explanation.~~

~~In contrast,~~It is interesting to note that the ~~relatively stable~~ $\delta^{34}S$ isotopic signature of HAS is relatively stable (except one outlier value of -25.9 ‰) over depth compared to CRS and

Formatted: Indent: First line: 1,25 cm
Formatted: Not Highlight
Formatted: Not Highlight
Formatted: Not Highlight
Formatted: Not Highlight
Formatted: Not Highlight
Formatted: Not Highlight
Formatted: Not Highlight
Formatted: Subscript
Formatted: Not Highlight
Formatted: Not Highlight
Formatted: Not Highlight
Formatted: Indent: First line: 0 cm
Formatted: Indent: First line: 1,25 cm

AVS. This suggests that humic acid-bound sulfur is overwhelmingly formed in surface sediments and not prone to significant alteration after formation and burial. ~~This implies that~~In contrast to inorganic sulfur, humic acid-bound S is extremely resistant to chemical or microbial transformation. Nonetheless, the presence of elemental sulfur and free sulfide leads to formation of polysulfides which are extremely reactive with organic matter and can confer the $\delta^{34}S$ signature of sulfate reduction to organic S (Amrani and Aizenshtat, 2004)

CONCLUSION

Here we report the first biogeochemical and isotopic data on sulfur cycling in the ancient (up to 13.5 kya) ~~lake~~ sediments of Lake Cadagno~~.~~, which represent an intermediate case study between the marine and low-sulfate lake sediments. In addition to confirming the rapid sulfurization of organic matter~~,~~, we have documented two separate zones of ~~CRS~~ reduced sulfur formation within the same sediment column~~, t~~. The deeper one is ~~driven~~ fed by sulfate-rich, oxidizing groundwater driving sulfide oxidation and leaving an isotopic imprint on newly formed sulfur minerals. ~~Surprising similarities in S-isotope fractionation patterns in surface and deep sediments are likely determined by closed-system S-isotope fractionation despite the very different sources of organic matter, sulfate concentrations, and sulfur-cycling microbial communities~~Consistent isotope offsets between pools of reduced sulfur (HAS, AVS, and CRS) are thus governed by the timing of their formation.

In other environments, the reduction of sulfate diffusing from terrestrial aquifers (Porowski et al., 2019), submarine groundwater discharge sites (McAllister et al., 2015) and even deep crustal aquifers (Engelen et al., 2008), ~~or evaporated sea-water trapped in the sediments (Vengosh et al., 1994) could essentially form new CRS with authigenic~~result in overprinting of new $\delta^{34}S$ ~~signatures potentially different from surface~~on buried sediments. This phenomenon

Formatted: English (United States)

Formatted: English (United States)

Formatted: English (United States)

Formatted: English (United States)

might actually be widespread as submarine groundwater seepage is a common, understudied phenomenon and the basaltic ocean crust is the largest aquifer system on Earth.

Deep sulfur cycling in Lake Cadagno appears to be driven by a diverse, and uncultivated biosphere, as most *dsr*B lineages recovered here belong to novel taxa whose role in sulfur and carbon cycling has yet to be revealed. These microorganisms, such as Chloroflexota, are not classical sulfate-reducing bacteria that have been characterized thus far in the laboratory and much is yet to be understood about their metabolisms. Nonetheless, the recovery of sulfur oxidation genes (*sox*B) from presumably anoxic surface sediments and sulfate reduction genes (*dsr*B) from sulfate-depleted deep sediments opens new questions about deep sources of oxidants which could drive continued sulfur-cycling in such reducing environments.

ACKNOWLEDGEMENTS

We thank the entire 2019 Cadagno sampling crew for assistance in the field, and especially the Alpine Biology Center Foundation (Switzerland) for use of its research facilities. We also acknowledge Iso Christl, Rachele Ossola, and Jorge Spangenberg for their support with chemical analyses. Longhui Deng. was sponsored by the Shanghai Pujiang Program (22PJ1404800). This study was supported by the Swiss National Science Foundation (SNF) grant No. 182096 (M.A.L.).

COMPETING INTERESTS

At least one author is a member of the editorial board of *Biogeosciences*.

DATA AVAILABILITY

*dsr*B gene sequences have been deposited in the NCBI database under Bioproject number PRJNA991470. All other raw data has been deposited in SWISSUbase under study number 20541.

4.5. AUTHOR CONTRIBUTIONS

JSB performed sediment sampling and chemical analyses, synthesized the data and wrote the manuscript. PCR and LD performed microbial community analyses and interpretations under supervision of CM. SB provided S-isotope data from 1991 and 2019. HV and MM performed sediment sampling and sedimentological characterizations and dating. All co-authors contributed to revision and editing of this manuscript and MAL supervised this project.

REFERENCES

Amrani A. and Aizenshtat Z. (2004) Mechanisms of sulfur introduction chemically controlled: δ34S imprint. *Organic Geochemistry* **35**, 1319–1336.

Anantharaman K., Hausmann B., Jungbluth S. P., Kantor R. S., Lavy A., Warren L. A., Rappé M. S., Pester M., Loy A., Thomas B. C. and Banfield J. F. (2018) Expanded diversity of microbial groups that shape the dissimilatory sulfur cycle. *ISME J* **12**, 1715–1728.

Anderson T. F. and Pratt L. M. (1995) Isotopic Evidence for the Origin of Organic Sulfur and Elemental Sulfur in Marine Sediments. In *Geochemical Transformations of Sedimentary Sulfur* ACS Symposium Series. American Chemical Society. pp. 378–396.

Baloza M., Henkel S., Geibert W., Kasten S. and Holtappels M. (2022) Benthic Carbon Remineralization and Iron Cycling in Relation to Sea Ice Cover Along the Eastern Continental Shelf of the Antarctic Peninsula. *Journal of Geophysical Research: Oceans* **127**, e2021JC018401.

Berg J. S., Lepine M., Laymand E., Han X., Vogel H., Morlock M. A., Gajendra N., Gilli A., Bernasconi S. M., Schubert C. J., Su G. and Lever M. A. (2022) Ancient and Modern Geochemical Signatures in the 13,500-Year Sedimentary Record of Lake Cadagno. *Frontiers in Earth Science* **9**.

Bernasconi S. M., Meier I., Wohlwend S., Brack P., Hochuli P. A., Bläsi H., Wortmann U. G. and Ramseyer K. (2017) An evaporite-based high-resolution sulfur isotope record of Late Permian and Triassic seawater sulfate. *Geochimica et Cosmochimica Acta* **204**, 331–349.

Birch L., Hanselmann K. W. and Bachofen R. (1996) Heavy metal conservation in Lake Cadagno sediments: Historical records of anthropogenic emissions in a meromictic alpine lake. *Water Research* **30**, 679–687.

Bowles M. W., Mogollón J. M., Kasten S., Zabel M. and Hinrichs K.-U. (2014) Global rates of marine sulfate reduction and implications for sub–sea-floor metabolic activities. *Science* **344**, 889–891.

Bradley A. S., Leavitt W. D., Schmidt M., Knoll A. H., Girguis P. R. and Johnston D. T. (2016) Patterns of sulfur isotope fractionation during microbial sulfate reduction. *Geobiology* **14**, 91–101.

Brüchert V. (1998) Early diagenesis of sulfur in estuarine sediments: the role of sedimentary humic and fulvic acids. *Geochimica et Cosmochimica Acta* **62**, 1567–1586.

Formatted: Numbered + Level: 1 + Numbering Style: 1, 2, 3, … + Start at: 4 + Alignment: Left + Aligned at: 0 cm + Indent at: 0,63 cm

Formatted: English (United States)

Formatted: English (United States)

Brunner B., Arnold G. L., Røy H., Müller I. A. and Jørgensen B. B. (2016) Off Limits: Sulfate below the Sulfate-Methane Transition. *Front. Earth Sci.* **4**.

Brunner B. and Bernasconi S. M. (2005) A revised isotope fractionation model for dissimilatory sulfate reduction in sulfate reducing bacteria. *Geochimica et Cosmochimica Acta* **69**, 4759–4771.

Bryant R. N., Houghton J. L., Jones C., Pasquier V., Halevy I. and Fike D. A. (2023) Deconvolving microbial and environmental controls on marine sedimentary pyrite sulfur isotope ratios. *Science* **382**, 912–915.

Canfield D. E., Farquhar J. and Zerkle A. L. (2010) High isotope fractionations during sulfate reduction in a low-sulfate euxinic ocean analog. *Geology* **38**, 415–418.

Cypionka H., Smock A. M. and Böttcher M. E. (1998) A combined pathway of sulfur compound disproportionation in Desulfovibrio desulfuricans. *FEMS Microbiology Letters* **166**, 181–186.

Damsté J. S. and De Leeuw J. W. (1990) Analysis, structure and geochemical significance of organically-bound sulphur in the geosphere: State of the art and future research. *Organic Geochemistry* **16**, 1077–1101.

Damste J. S., Kok M. D., Koster J. and Schouten S. (1998) Sulfurized carbohydrates: an important sedimentary sink for organic carbon? *Earth and Planetary Science Letters* **164**, 7–13.

Damsté J. S., Kok M. D., Köster J. and Schouten S. (1998) Sulfurized carbohydrates: an important sedimentary sink for organic carbon? *Earth and Planetary Science Letters* **164**, 7–13.

David M. B. and Mitchell M. J. (1985) Sulfur constituents and cycling in waters, seston, and sediments of an oligotrophic lake. *Limnology and Oceanography* **30**, 1196–1207.

Deng L., Meile C., Fiskal A., Bölsterli D., Han X., Gajendra N., Dubois N., Bernasconi S. M. and Lever M. A. (2022) Deposit-feeding worms control subsurface ecosystem functioning in intertidal sediment with strong physical forcing. *PNAS Nexus* **1**, pgac146.

Detmers J., Brüchert V., Habicht K. S. and Kuever J. (2001) Diversity of Sulfur Isotope Fractionations by Sulfate-Reducing Prokaryotes. *Appl. Environ. Microbiol.* **67**, 888–894.

Eglinton T. I., Irvine J. E., Vairavamurthy A., Zhou W. and Manowitz B. (1994) Formation and diagenesis of macromolecular organic sulfur in Peru margin sediments. *Organic Geochemistry* **22**, 781–799.

Engelen B., Ziegelmüller ,Katja, Wolf ,Lars, Köpke ,Beate, Gittel ,Antje, Cypionka ,Heribert, Treude ,Tina, Nakagawa ,Satoshi, Inagaki ,Fumio, Lever ,Mark Alexander and and Steinsbu B. O. (2008) Fluids from the Oceanic Crust Support Microbial Activities within the Deep Biosphere. *Geomicrobiology Journal* **25**, 56–66.

Ferdelman T. G., Church T. M. and Luther G. W. (1991) Sulfur enrichment of humic substances in a Delaware salt marsh sediment core. *Geochimica et Cosmochimica Acta* **55**, 979–988.

Fike D. A., Bradley A. S. and Rose C. V. (2015) Rethinking the Ancient Sulfur Cycle. *Annual Review of Earth and Planetary Sciences* **43**, 593–622.

Fiskal A., Deng L., Michel A., Eickenbusch P., Han X., Lagostina L., Zhu R., Sander M., Schroth M. H., Bernasconi S. M., Dubois N. and Lever M. A. (2019) Effects of eutrophication on sedimentary organic carbon cycling in five temperate lakes. *Biogeosciences* **16**, 3725–3746.

Fossing H. and Jørgensen B. B. (1989) Measurement of bacterial sulfate reduction in sediments: Evaluation of a single-step chromium reduction method. *Biogeochemistry* **8**, 205–222.

Gajendra N., Berg J. S., Vogel H., Deng L., Wolf S. M., Bernasconi S. M., Dubois N., Schubert C. J. and Lever M. A. (2023) Carbohydrate compositional trends throughout Holocene sediments of an alpine lake (Lake Cadagno). *Front. Earth Sci.* **11**, 1047224.

Goldhaber M. B. and Kaplan I. R. (1975) Controls and consequences of sulfate reduction rates in recent marine sediments. *Soil Science* **119**, 42.

Goldhaber M. B. and Kaplan I. R. (1980) Mechanisms of sulfur incorporation and isotope fractionation during early diagenesis in sediments of the gulf of California. *Marine Chemistry* **9**, 95–143.

Habicht K. S. and Canfield D. E. (1997) Sulfur isotope fractionation during bacterial sulfate reduction in organic-rich sediments. *Geochimica et Cosmochimica Acta* **61**, 5351–5361.

Hansel C. M., Lentini C. J., Tang Y., Johnston D. T., Wankel S. D. and Jardine P. M. (2015) Dominance of sulfur-fueled iron oxide reduction in low-sulfate freshwater sediments. *ISME J* **9**, 2400–2412.

Hartmann M. and Nielsen H. (2012) δ34S values in recent sea sediments and their significance using several sediment profiles from the western Baltic Sea. *Isotopes in Environmental and Health Studies* **48**, 7–32.

Hashimoto Y., Shimamura S., Tame A., Sawayama S., Miyazaki J., Takai K. and Nakagawa S. (2022) Physiological and comparative proteomic characterization of Desulfolithobacter dissulfuricans gen. nov., sp. nov., a novel mesophilic, sulfur-disproportionating chemolithoautotroph from a deep-sea hydrothermal vent. *Front. Microbiol.* **13**.

Hebting Y., Schaeffer P., Behrens A., Adam P., Schmitt G., Schneckenburger P., Bernasconi S. M. and Albrecht P. (2006) Biomarker Evidence for a Major Preservation Pathway of Sedimentary Organic Carbon. *Science* **312**, 1627–1631.

Holmkvist L., Kamyshny A., Vogt C., Vamvakopoulos K., Ferdelman T. G. and Jørgensen B. B. (2011) Sulfate reduction below the sulfate–methane transition in Black Sea sediments. *Deep Sea Research Part I: Oceanographic Research Papers* **58**, 493–504.

Huc A. Y. and Durand B. M. (1977) Occurrence and significance of humic acids in ancient sediments. *Fuel* **56**, 73–80.

Jochum L. M., Chen X., Lever M. A., Loy A., Jørgensen B. B., Schramm A. and Kjeldsen K. U. (2017) Depth Distribution and Assembly of Sulfate-Reducing Microbial Communities in Marine Sediments of Aarhus Bay. *Appl. Environ. Microbiol.* **83**.

Jørgensen B. B. (1982) Mineralization of organic matter in the sea bed—the role of sulphate reduction. *Nature* **296**, 643–645.

Formatted: English (United States)

739 Jørgensen B. B., Böttcher M. E., Lüschen H., Neretin L. N. and Volkov I. I. (2004) Anaerobic methane
740 oxidation and a deep H2S sink generate isotopically heavy sulfides in Black Sea sediments 1.
741 *Geochimica et Cosmochimica Acta* **68**, 2095–2118.

742 Kallmeyer J., Ferdelman T. G., Weber A., Fossing H. and Jørgensen B. B. (2004) A cold chromium
743 distillation procedure for radiolabeled sulfide applied to sulfate reduction measurements.
744 *Limnology and Oceanography: Methods* **2**, 171–180.

745 Kaplan I. R. and Rittenberg S. C. Y. 1964 (1964) Microbiological Fractionation of Sulphur Isotopes.
746 *Microbiology* **34**, 195–212.

747 Klein M., Friedrich M., Roger A. J., Hugenholtz P., Fishbain S., Abicht H., Blackall L. L., Stahl D. A. and
748 Wagner M. (2001) Multiple Lateral Transfers of Dissimilatory Sulfite Reductase Genes
749 between Major Lineages of Sulfate-Reducing Prokaryotes. *Journal of Bacteriology* **183**, 6028–
750 6035.

751 Kok M. D., Schouten S. and Sinninghe Damsté J. S. (2000) Formation of insoluble, nonhydrolyzable,
752 sulfur-rich macromolecules via incorporation of inorganic sulfur species into algal
753 carbohydrates. *Geochimica et Cosmochimica Acta* **64**, 2689–2699.

754 Lever M. A., Rouxel O., Alt J. C., Shimizu N., Ono S., Coggon R. M., Shanks W. C., Lapham L., Elvert M.,
755 Prieto-Mollar X., Hinrichs K.-U., Inagaki F. and Teske A. (2013) Evidence for Microbial Carbon
756 and Sulfur Cycling in Deeply Buried Ridge Flank Basalt. *Science* **339**, 1305–1308.

757 Lever M. A., Torti A., Eickenbusch P., Michaud A. B., Šantl-Temkiv T. and Jørgensen B. B. (2015) A
758 modular method for the extraction of DNA and RNA, and the separation of DNA pools from
759 diverse environmental sample types. *Front. Microbiol.* **6**.

760 Liu R., Wei X., Song W., Wang L., Cao J., Wu J., Thomas T., Jin T., Wang Z., Wei W., Wei Y., Zhai H., Yao
761 C., Shen Z., Du J. and Fang J. (2022) Novel Chloroflexi genomes from the deepest ocean
762 reveal metabolic strategies for the adaptation to deep-sea habitats. *Microbiome* **10**, 75.

763 Losher A. (1989) The sulfur cycle in freshwater lake sediments and implications for the use of C/S
764 ratios as indicators of past environmental changes. *Doctoral dissertation, ETH Zurich*.

765 Luther G. W. (1991) Pyrite synthesis via polysulfide compounds. *Geochimica et Cosmochimica Acta*
766 **55**, 2839–2849.

767 Maynard J. B. (1980) Sulfur isotopes of iron sulfides in Devonian-Mississippian shales of the
768 Appalachian basin: control by rate of sedimentation. *Am. J. Sci.; (United States)* **280:8**.

769 McAllister S. M., Barnett J. M., Heiss J. W., Findlay A. J., MacDonald D. J., Dow C. L., Luther III G. W.,
770 Michael H. A. and Chan C. S. (2015) Dynamic hydrologic and biogeochemical processes drive
771 microbially enhanced iron and sulfur cycling within the intertidal mixing zone of a beach
772 aquifer. *Limnology and Oceanography* **60**, 329–345.

773 Mehrshad M., Rodriguez-Valera F., Amoozegar M. A., López-García P. and Ghai R. (2018) The
774 enigmatic SAR202 cluster up close: shedding light on a globally distributed dark ocean
775 lineage involved in sulfur cycling. *ISME J* **12**, 655–668.

776 Meyer B., Imhoff J. F. and Kuever J. (2007) Molecular analysis of the distribution and phylogeny of
777 the soxB gene among sulfur-oxidizing bacteria – evolution of the Sox sulfur oxidation enzyme
778 system. *Environmental Microbiology* **9**, 2957–2977.

Mitchell M. J., Landers D. H. and Brodowski D. F. (1981) Sulfur constituents of sediments and their relationship to lake acidification. *Water Air Soil Pollut* **16**, 351–359.

Müller A. L., Kjeldsen K. U., Rattei T., Pester M. and Loy A. (2015) Phylogenetic and environmental diversity of DsrAB-type dissimilatory (bi)sulfite reductases. *The ISME Journal* **9**, 1152–1165.

Nriagu J. O. and Soon Y. K. (1985) Distribution and isotopic composition of sulfur in lake sediments of northern Ontario. *Geochimica et Cosmochimica Acta* **49**, 823–834.

Ono S., Sim M. S. and Bosak T. (2014) Predictive isotope model connects microbes in culture and nature. *Proceedings of the National Academy of Sciences* **111**, 18102–18103.

Orr W. L. and Damsté J. S. (1990) Geochemistry of Sulfur in Petroleum Systems. In *Geochemistry of Sulfur in Fossil Fuels* ACS Symposium Series. American Chemical Society. pp. 2–29.

Pellerin A., Antler G., Røy H., Findlay A., Beulig F., Scholze C., Turchyn A. V. and Jørgensen B. B. (2018a) The sulfur cycle below the sulfate-methane transition of marine sediments. *Geochimica et Cosmochimica Acta* **239**, 74–89.

Pellerin A., Antler G., Røy H., Findlay A., Beulig F., Scholze C., Turchyn A. V. and Jørgensen B. B. (2018b) The sulfur cycle below the sulfate-methane transition of marine sediments. *Geochimica et Cosmochimica Acta* **239**, 74–89.

Pester M., Knorr K.-H., Friedrich M. W., Wagner M. and Loy A. (2012) Sulfate-reducing microorganisms in wetlands – fameless actors in carbon cycling and climate change. *Front. Microbiol.* **3**.

Porowski A., Porowska D. and Halas S. (2019) Identification of Sulfate Sources and Biogeochemical Processes in an Aquifer Affected by Peatland: Insights from Monitoring the Isotopic Composition of Groundwater Sulfate in Kampinos National Park, Poland. *Water* **11**, 1388.

Putschew A., Scholz-Böttcher B. M. and Rullkötter J. (1996) Early diagenesis of organic matter and related sulphur incorporation in surface sediments of meromictic Lake Cadagno in the Swiss Alps. *Organic Geochemistry* **25**, 379–390.

Raven M. R., Crockford P. W., Hodgskiss M. S. W., Lyons T. W., Tino C. J. and Webb S. M. (2023) Organic matter sulfurization and organic carbon burial in the Mesoproterozoic. *Geochimica et Cosmochimica Acta* **347**, 102–115.

Raven M. R., Sessions A. L., Fischer W. W. and Adkins J. F. (2016) Sedimentary pyrite δ34S differs from porewater sulfide in Santa Barbara Basin: Proposed role of organic sulfur. *Geochimica et Cosmochimica Acta* **186**, 120–134.

Rudd J. W. M., Kelly C. A. and Furutani A. (1986) The role of sulfate reduction in long term accumulation of organic and inorganic sulfur in lake sediments1. *Limnology and Oceanography* **31**, 1281–1291.

Rudnicki M. D., Elderfield H. and Spiro B. (2001) Fractionation of sulfur isotopes during bacterial sulfate reduction in deep ocean sediments at elevated temperatures. *Geochimica et Cosmochimica Acta* **65**, 777–789.

Formatted: English (United States)

Schubert C. J., Vazquez F., Lösekann-Behrens T., Knittel K., Tonolla M. and Boetius A. (2011) Evidence for anaerobic oxidation of methane in sediments of a freshwater system (Lago di Cadagno). *FEMS Microbiology Ecology* **76**, 26–38.

Schwarcz H. P. and Burnie S. W. (1973) Influence of sedimentary environments on sulfur isotope ratios in clastic rocks: a review. *Mineral. Deposita* **8**, 264–277.

Sim M. S., Bosak T. and Ono S. (2011) Large Sulfur Isotope Fractionation Does Not Require Disproportionation. *Science* **333**, 74–77.

Sinninghe Damsté J. S., Eglinton T. I., Rijpstra W. I. C. and de Leeuw J. W. (1990) Characterization of Organically Bound Sulfur in High-Molecular-Weight, Sedimentary Organic Matter Using Flash Pyrolysis and Raney Ni Desulfurization. In *Geochemistry of Sulfur in Fossil Fuels* ACS Symposium Series. American Chemical Society. pp. 486–528.

Slobodkin A. I. and Slobodkina G. B. (2019) Diversity of Sulfur-Disproportionating Microorganisms. *Microbiology* **88**, 509–522.

Steingruber S. M., Bernasconi S. M. and Valenti G. (2020) Climate Change-Induced Changes in the Chemistry of a High-Altitude Mountain Lake in the Central Alps. *Aquat Geochem*.

Stookey L. L. (1970) Ferrozine---a new spectrophotometric reagent for iron. *ACS Publications*.

Treude T., Krause S., Maltby J., Dale A. W., Coffin R. and Hamdan L. J. (2014) Sulfate reduction and methane oxidation activity below the sulfate-methane transition zone in Alaskan Beaufort Sea continental margin sediments: Implications for deep sulfur cycling. *Geochimica et Cosmochimica Acta* **144**, 217–237.

Urban N. R., Ernst K. and Bernasconi S. (1999) Addition of sulfur to organic matter during early diagenesis of lake sediments. *Geochimica et Cosmochimica Acta* **63**, 837–853.

Vuillemin A., Kerrigan Z., D'Hondt S. and Orsi W. D. (2020) Exploring the abundance, metabolic potential and gene expression of subseafloor Chloroflexi in million-year-old oxic and anoxic abyssal clay. *FEMS Microbiology Ecology* **96**, fiaa223.

Wasmund K., Mußmann M. and Loy A. (2017) The life sulfuric: microbial ecology of sulfur cycling in marine sediments. *Environmental Microbiology Reports* **9**, 323–344.

Wasmund K., Schreiber L., Lloyd K. G., Petersen D. G., Schramm A., Stepanauskas R., Jørgensen B. B. and Adrian L. (2014) Genome sequencing of a single cell of the widely distributed marine subsurface Dehalococcoidia, phylum Chloroflexi. *ISME J* **8**, 383–397.

Werne J. P., Lyons T. W., Hollander D. J., Formolo M. J. and Sinninghe Damsté J. S. (2003) Reduced sulfur in euxinic sediments of the Cariaco Basin: sulfur isotope constraints on organic sulfur formation. *Chemical Geology* **195**, 159–179.

Werne J. P., Lyons T. W., Hollander D. J., Schouten S., Hopmans E. C. and Sinninghe Damsté J. S. (2008) Investigating pathways of diagenetic organic matter sulfurization using compound-specific sulfur isotope analysis. *Geochimica et Cosmochimica Acta* **72**, 3489–3502.

Wirth S. B., Gilli A., Niemann H., Dahl T. W., Ravasi D., Sax N., Hamann Y., Peduzzi R., Peduzzi S., Tonolla M., Lehmann M. F. and Anselmetti F. S. (2013) Combining sedimentological, trace metal (Mn, Mo) and molecular evidence for reconstructing past water-column redox

conditions: The example of meromictic Lake Cadagno (Swiss Alps). *Geochimica et Cosmochimica Acta* **120**, 220–238.

Wortmann U. G., Bernasconi S. M. and Böttcher M. E. (2001) Hypersulfidic deep biosphere indicates extreme sulfur isotope fractionation during single-step microbial sulfate reduction. *Geology* **29**, 647–650.